Elastic asymmetries analysis for experiment E94010 (V.1)

Alexandre Deur[*], Steffen Jensen[†]

December 18, 2000

Abstract

The two sets of elastic data taken during the experiment E94010 are analysed. The comparison between the experimental asymmetries and the simulated ones provides a check of our understanding of the detectors, acceptance, target and beam polarimetries. Experimental and simulated results are in agreement within the error bars. The systematic error achieved is of the order of 6% (preliminary estimate).

This note also details the deadtime fluctuation problems, its implication on the asymmetry measurement, how it is corrected and the validity of the correction.

Contents

[*]Jefferson Lab & LPC/Université Blaise Pascal, deurpam@jlab.org
[†]California Institute of Technology, steffen@general.krl.caltech.edu

1 Introduction.

^{3}He elastic data at incident energies of 0.862 GeV (Q^2= 0.053 GeV^2) and 1.72 GeV (Q^2=0.21 GeV^2) were taken during the experiment E94010. The purpose was to check our control of the experimental apparatus. (^{3}He elastic form factors are well known experimentally and well fitted). This data provides also a beam energy measurement. (E94010 does not have reliable energy measurements at these two energies). This note presents our results on the elastic asymmetries.

2 Analysis.

2.1 Data.

$\overrightarrow{e}(^3He,e')X$ Elastic data was collected at 0.862 GeV and 1.72 GeV. For both energies the "electron" spectrometer angle is $+15.503^o$ and the "hadron" arm[1] angle is -15.528^o. Data at 1.72 GeV was first taken at the beginning of the experiment: runs 1580 to 1587. These runs are not analysed here because of unreliable charge asymmetry measurement. Data analysed for this paper is summarised in the table below:

Energy	First run	Last run	Momentum setting	Target spin
1.718 GeV	1768	1778	1730 GeV/c	parallel
1.717 GeV	2316	2319	1730 GeV/c	parallel
0.862 GeV	2836	2841	0.860 GeV/c	parallel
0.862 GeV	2842	2844	0.873 GeV/c	perpendicular
0.862 GeV	2845	2851	0.860 GeV/c	parallel
0.862 GeV	2852	2854	0.834 GeV/c	perpendicular
0.862 GeV	2855	2865	0.860 GeV/c	parallel

For 1.72 GeV both arms shared one data acquisition.
the 0.862 GeV data where taken with two independent DAQ.

2.2 Cuts.

Cuts select the electrons scattering elastically from ^{3}He:

[1] The "hadron" arm detect electron too: e94010 is an inclusive experiment.

- Particle identification cuts: 2 dimensional cut on shower and preshower for the electron arm removes pions[2]. The hadron arm shower has a 1 dimensional cut. Cerenkov cuts were applied to both arms.
- Geometrical cuts: theta_target, phi_target, y_target and $\triangle$P remove electrons scattered from the target glass windows.
- an w (invariant mass) cut selects the elastic reaction[3].

The cut sizes are given in the table below.

-50<θ_{target}<50 mRd
-30<φ_{target}<30 mRd
-5.5<y_{target}<4 cm
-1<$w - M_{He3}$<4 MeV
-3.5<dp/p<2.7

The asymmetry cut dependency (in case of non-elastic events contamination, for ex. the "low energy events" mentioned in ref [1]) was checked by making the two dimensional particle identification cut tighter and tighter. The result is plotted in Fig 2 and shows no cut dependency.

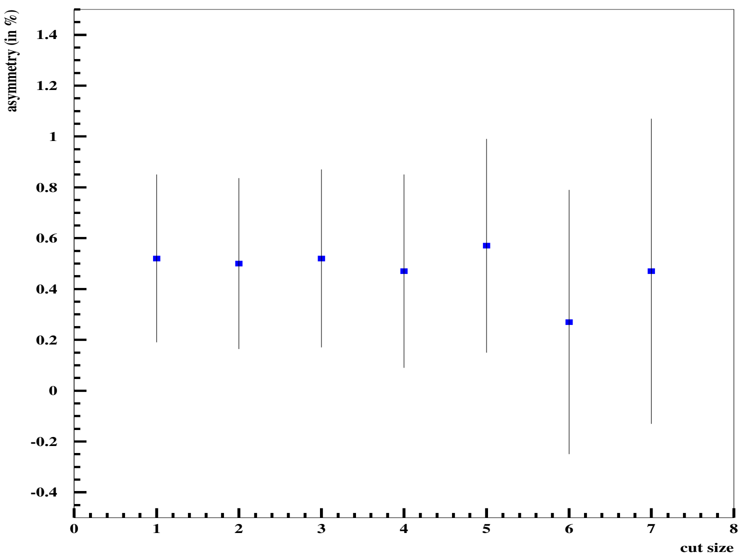

Fig. 2. Asymmetry dependence on the cuts. The vertical axis is the asymmetry value. The farther on the horizontal axis, the tighter the particle

[2]Elastic is below the pion threshold. Pion contamination is negligible

[3]A one dimensional cut in w should be enough to select the elastic peak. However due to an hysteresis problem w is slightly correlated with θ_{target}. We applied a 2 dimensional cut in the plan (w, θ_{target}) in order to take care of this the consequence of such correlation (possible contamination from the quasi-elastic). It was found that the 1 dimensional -1<$w - M_{He3}$<4 MeV cut does not let in a significant amount of contamination.

identification cut is. The asymmetry is stable at the beginning and eventually begins to jump as the statistic decreases.

2.3 Trigger Inefficiency Correction.

The trigger inefficiency degraded during the experimental run. As it depends of the paddle and of the interaction position in the paddle, it is correlated with the electron scattering angle. Since the asymmetry varies significantly in the spectrometer acceptance we have to correct for this inefficiency. As far as this analysis is concerned, the trigger inefficiency is found to have a negligible effect.

2.4 Charge Asymmetry.

The number of incoming electrons of helicity plus is different from the number of helicity minus ones. This creates a false asymmetry (charge asymmetry). The correction formula is:

$$A = \frac{N^+/q^+ - N^-/q^-}{N^+/q^+ + N^-/q^-}$$

Where N^i is the number of helicity i events and q^i the corresponding integrated charge.

This asymmetry can be due to:

1. A different number of helicity plus pulses and helicity minus pulses coming on the target

2. A difference in the number of electron within the helicity plus pulses and within helicity minus pulses.

The first case does not cause a large charge asymmetry: To cancel systematic effects the pulse is delivered as following: The first pulse is chosen pseudo-randomly (i.e following an apparent random but still predictable choice) while the second one is chosen with the opposite helicity. The next pulse is then again chosen pseudo-randomly and so on. Fig. 8 of section 4 shows that this pattern was working fine during the 0.862 GeV/c elastic runs. A difference in number of pulses could come from the beginning or the end of the run when the run starts or ends in the middle of a pulse. This charge asymmetry is small if the run is reasonably long (we had 1 second pulses for E94010). Charge asymmetry could also come from beam trips but on the average the asymmetry should cancel out since beam trips are uncorrelated with the helicity (it's often a cavity trip).

The charge asymmetry is mainly due to the second case. The laser light that shines the polarised source photocathode does not have the same intensity in its different polarisations state. Consequently the number of extracted electrons of helicity plus is different from the ones of helicity minus. This charge asymmetry was kept as low as possible (cf section 5).

2.5 Acceptance Effect Correction.

The cross section and asymmetry vary in the spectrometer finite acceptance. These variations, within a simple rectangular acceptance model, decrease the simulated asymmetry by 10% in respect to simulation done with a pointlike acceptance model. A more exact acceptance is simulated using the Monte Carlo MCE94010 (ref [2]). This makes the total correction to be 12 %.

2.6 Nitrogen Correction.

Invariant mass spectra for E=0.862 GeV and E=1.72 GeV are shown in figures 3 and 4. The 1% nitrogen presents in the target cell is unpolarised and dilutes the asymmetries. The amount of contamination is computed in ref [4]. The dilution depends of the w cut chosen. With the cut defined in section 2.2 we have 0.7 % dilution for the 0.862 GeV elastic and 8.5 % for the 1.72 GeV elastic.

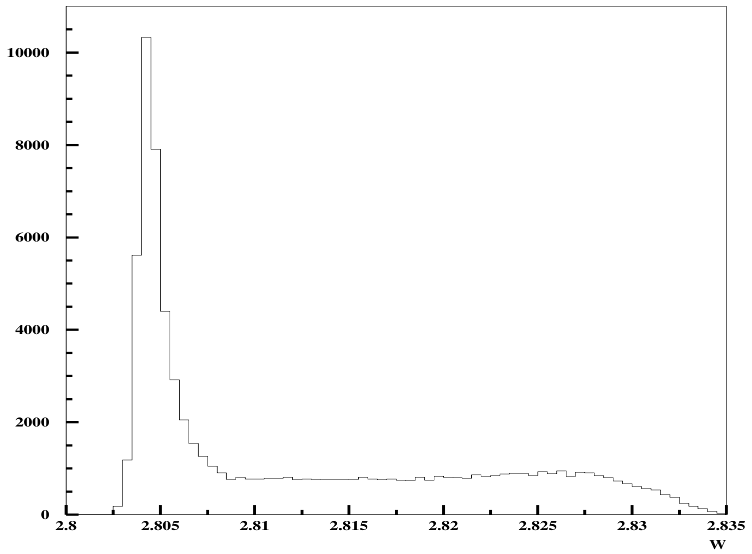

Fig w spectrum for E=0.862 GeV.

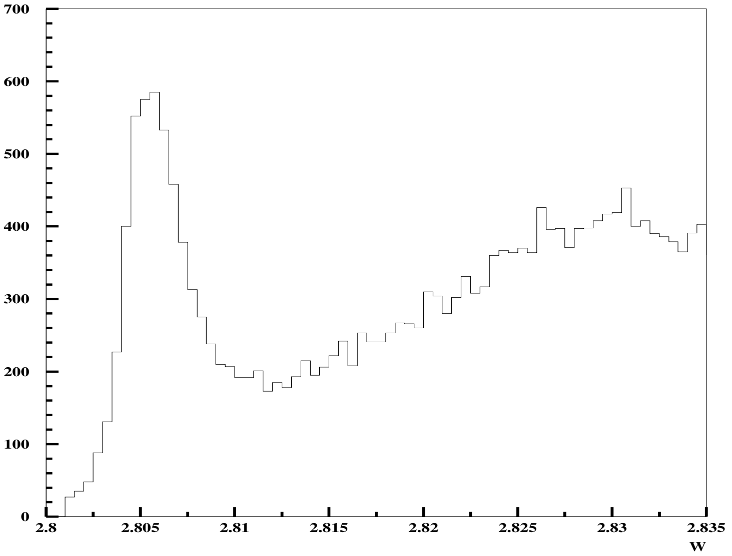

Fig. 4 W spectrum for E=1.72 GeV.

3 Radiative corrections.

3.1 Elastic Peak.

The internal radiative corrections consist of the vertex correction, vacuum polarisation, photon radiation from the particle lines and the self energy (the latter does not contribute). The external real radiative corrections are the energy loss and the bremsstrahlung (fig 6).

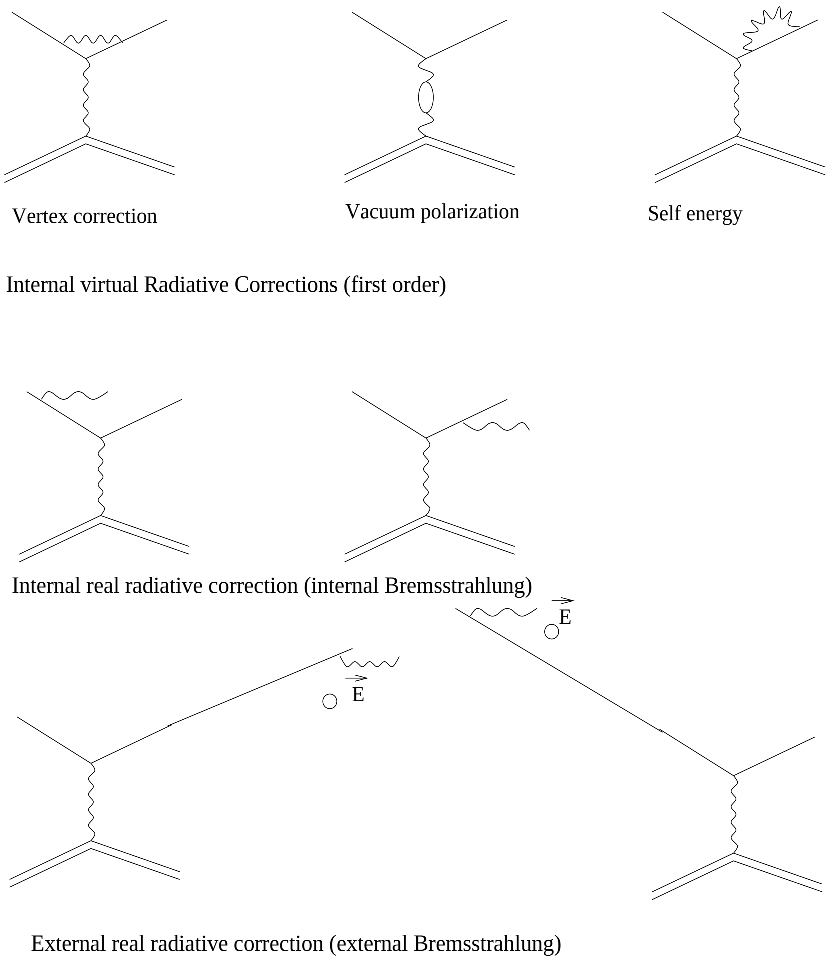

Fig 6. Internal and External radiative corrections.

if δ is the total radiative correction then:
σ_{exp}=$(1+\delta)$ σ_{born}
where σ denotes a cross section. Under the approximations below, the $1+\delta$ is helicity independent and will cancel out when the asymmetry is formed.

The assumptions are:

- The magnetic part of the vertex correction, the Landé Factor, is neglected in the vertex correction. It yields correction of at a few ppm level [3].
- Higher order radiative correction terms are not computed. According to the exponentiation theorem, the dominant part of these higher order terms will factorize.
- The electron energy loss is helicity independent (see section 3.2).
- The hadron energy loss is neglected regarding the heavy mass of the target.

Ref [3] calculates exactly the internal Bremsstrahlung in the case of a Proton for both E94010 kinematics. Hard Photon losses are taken into account. In this case the $(1+\delta\ )$ does not factorize and radiative corrections affect the elastic asymmetry. However a computation of this correction (for a proton target) for both E94010 elastic kinematics yield less than 0.1% correction on the elastic asymmetries [9].

3.2 Spin Flips Induced by Photon Emissions.

The asymmetry can be biased by a spin flip of the incoming electrons during a real photon emission (if the spin flips the contribution to the asymmetry takes the opposite sign and decreases absolute value of the final results). We will see a spin flip cannot happen: In the case of the peaking approximation, the photon is emitted in the electron direction. Taking the electron mass to be zero, the chiral symmetry makes the electron to keep the same helicity and no photons can be emitted (either it violates the chiral symmetry in the case of spin flip, or it violates the spin conservation in the case of photon emission without spin flip since there is no relative momentum between two particles going the same or opposite direction).[4] To summarise: The spin flips are not allowed in the chiral symmetry approximation so the electron energy losses do not shift the elastic asymmetry.

3.3 Radiative Correction in a Finite HRS Acceptance.

The bremsstrahlung before the scattering of the radiating electron changes the elastic kinematics. These events, with a different asymmetry, go in the radiative tail. Since the HRS has a finite acceptance, part of the elastic tail is seen and affects the asymmetry. This effect is naturally taken into account in our Monte Carlo. However the simulation shows that this phenomenon affect very little the average elastic asymmetry (a relative shift of 0.09 % for the 0.862 GeV kinematics).

4 Deadtime Correction.

4.1 Fluctuating Deadtime Effect.

4.1.1 Possible Causes of Trouble Coming from the Deadtime.

Deadtime comes mostly from computer data processing. It should be helicity independent. If so its effect factorizes and leaves the asymmetry unchanged (with larger statistical error bars). However for the reasons listed below, the data taking or deadtime can be helicity dependent.

- The physics asymmetry is large and the deadtime grows quickly with the DAQ rate. This effects is expected to be small according to the experimental raw asymmetry (a few percent). This effect is anyway corrected when we do the deadtime correction (see the end of this section).

[4] Then one may ask how a photon can be emitted at all ? It has to be emitted with a finite angle in respect to the electron direction. If the photon is emitted a little away from the electron direction, the chiral symmetry still imposes the helicity conservation. In the case of no spin flip and photon emission, the momentum conservation is done by the creation of the relative momentum between the electron and the photon. It is the only case where a photon can be radiated.

- The event size is different for helicity plus and helicity minus events. It will cause the computer to be more busy with the 1 second pulse of a helicity than with the other one. The deadtime in this case will be helicity correlated. This can happen if the pedestal suppression fails for one helicity[5]. If so he event length will be larger for one of the helicity.
- In the case of runs with instable deadtime, the average deadtime effect may not cancel out. It is not a helicity correlated deadtime but if it happens it requires the same kind of correction. Fig .7 shows a simulation result. It assumes a deadtime jumping to a random value at each pulse. It is totally uncorrelated with the helicity. The asymmetry fluctuation is plotted (centred to zero since we did not put no physics asymmetry in the simulation). We see that a jumping deadtime will make the experimental result to fluctuate in average by 0.3 % absolute but can lead sometime to much bigger fluctuations.

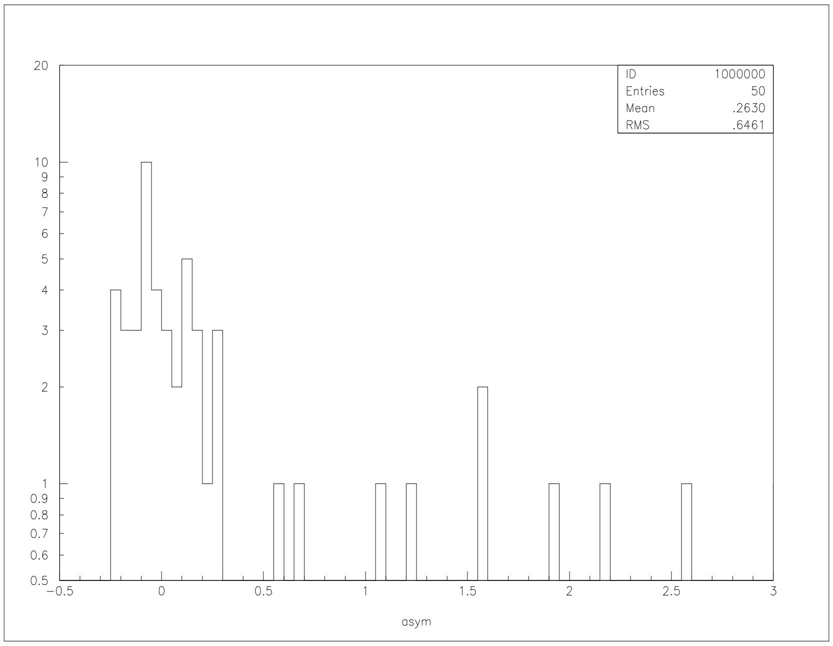

Fig. 7 asymmetry fluctuation due to an instable deadtime.

4.1.2 Pulse Distribution According to their content.

We call a pulse a pack of electron having the same helicity. According to the helicity flip frequency of 1 second, we can have 1 second or 2 second pulses only (cf section 2.4). Figure 8 plots the number of event in each pulse of a run. The first peak corresponds to a "pulse" from where only one electron is detected, the second peak to a 1 second pulse triggering 4000 events and the last peak to 2 second pulse generating 8000 triggers. The first peak may correspond to a wrong helicity affectation at the end of at the beginning of the pulse (otherwise

[5]The pedestal suppression removes all the detector ADCs low readings. cf ESPACE manual

if it was, say, in the middle we would have a 2000 events peak). It is harmless since it does not represent too much events[6]. The second peak corresponds to the case of a given helicity one second pulse surrounded by two opposite helicity pulses while the last peak correspond to the case of two pulses of the same helicity coming in a row. A deadtime fluctuation during a run will make the peak to spread to the left side since it decreases the number of events in one pulse by a fluctuating factor. If the spreads is the same for both helicities the effect will cancel out and will not affect the asymmetry.

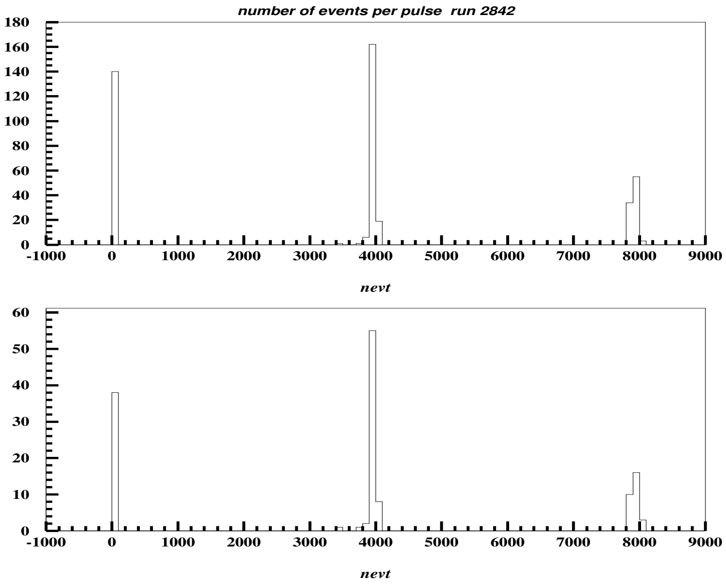

Fig 8. Number of events of the same helicity coming in a row. The top plot is for helicity minus while the bottom is for helicity plus (the peak highs are different for both helicities because we did not scan the same amount of events). The deadtime was stable during this run.

4.2 Asymmetry Without Deadtime Correction.

A plot (fig 9) of the E=0.862 GeV asymmetries without deadtime correction shows large jumps of the asymmetries that cannot be due to statistical fluctuation. They rather come from the deadtime fluctuations mentioned above as we are going to demonstrate.

[6]This problem is unsolved yet.

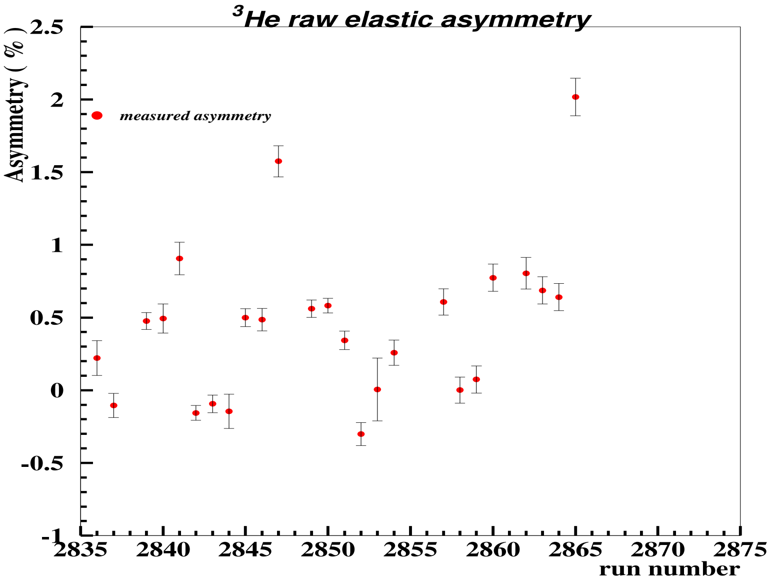

Fig 9. The E=0.862 GeV experimental asymmetries without deadtime corrections.

As the fluctuations are going both way (for ex runs 2855 and 2865 jump up while runs 2858 and 2859 jump down. It cannot be due to any systematic deadtime helicity correlation. A lifetime plot shows that the fluctuation is a deadtime-like effect (Fig 10): The lifetime for "hadron" arm events is defined as the trigger T3 (subject to computer deadtime) divided by the corresponding scaler (non subject to deadtime)[7]. If the deadtime was helicity independent or was cancelled out the lifetime for both helicity should be the same. It is not the case, especially with the runs 2837, 2846, 2855, 2858, 2859 and 2865.

[7] The livetime is usually defined with T3 multiplied by its prescaler.

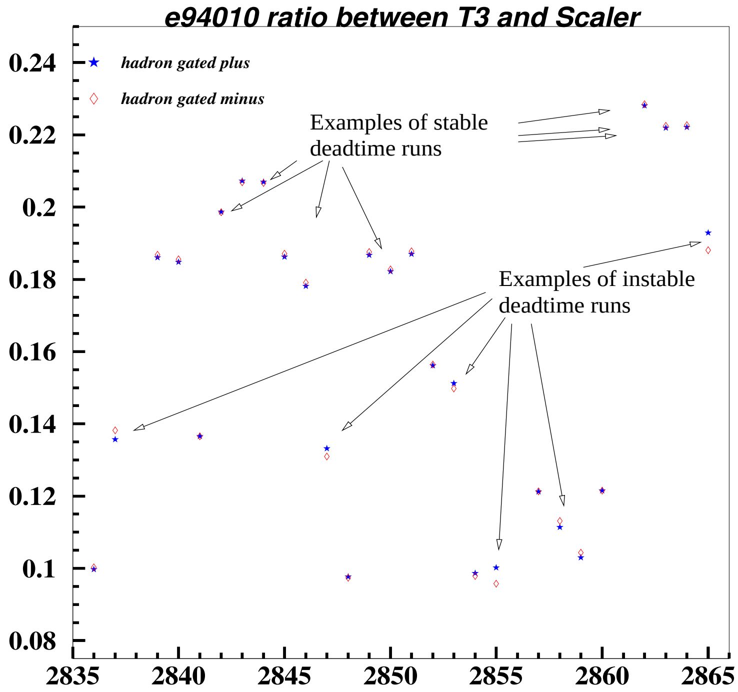

Fig10. Trigger 3 lifetime for helicity plus (stars) and minus trigger 3 (diamonds).

4.3 Asymmetry from Scalers

The asymmetries from scaler look stable (fig 11). We can see a correlation between the jumping asymmetry runs and the ones presenting a different ratio for both helicities in fig 10. The asymmetries without any cut are also plotted and are in good agreement with the scaler ones only if the two helicity plus and helicity minus lifetime match. The difference between fig 9 and 11 comes from the quasi-elastic events and the unpolarised events that are not cut out (pions, scattering off glass windows...) and dilute the asymmetries.

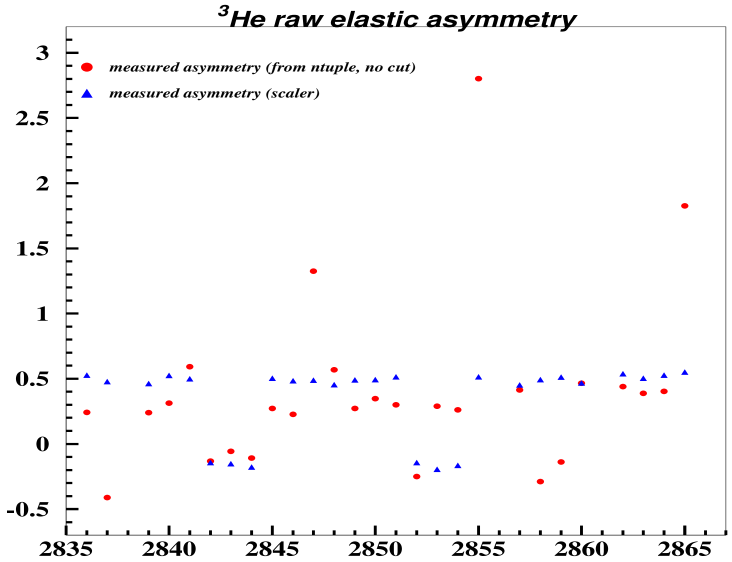

Fig 11 E=0.862 Asymmetries from scaler (triangles) and from coda events without any cut (circles).

4.4 Deadtime Evolution During a Run.

Fig 12 shows the deadtime for run 2837. During this period of data taking the deadtime was jumping to high values (as at the beginning of the run 2837) to be back to a stable value (as at the end of the run). The figures 13 and 14 show that the deadtime fluctuations affect the asymmetries. The spread is different for the two helicity leading to the observed jump of run 2837. Fig 15 shows the spread for the worst run (run 2855).

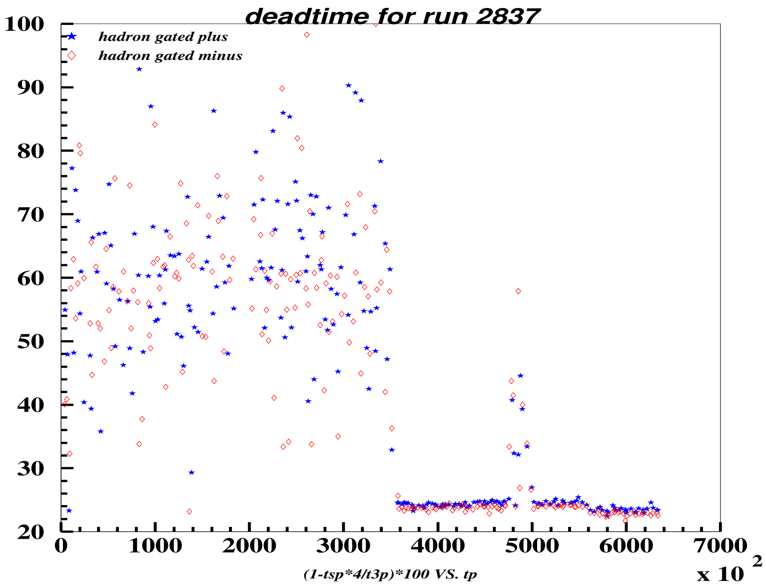

Fig 12. Deadtime for the run 2837. The horizontal is time (arbitrary unit) while the vertical is the deadtime.

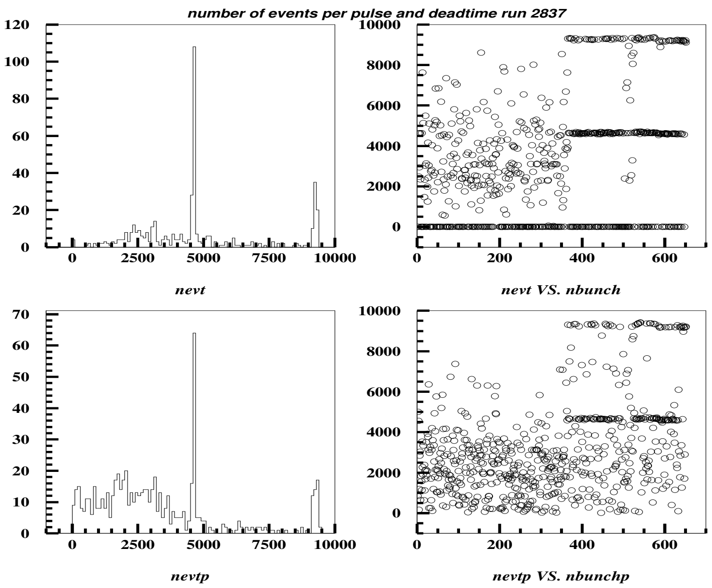

Fig 13 Number of events of the same helicity coming in a row for run 2837. The left top plot is for helicity minus while the left bottom is for helicity plus. The right plot shows the number of events in a pulse versus time (arbitrary unit) for each helicities.

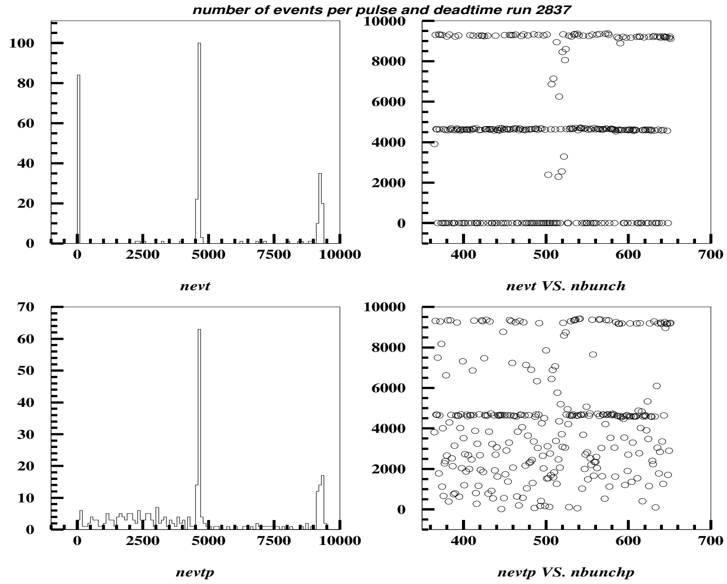

Fig 14. Same plots as fig 13 but with a cut on the deadtime. The jumping deadtime period is cut away. We can see the spreads of the peaks in the left plot is due to it.

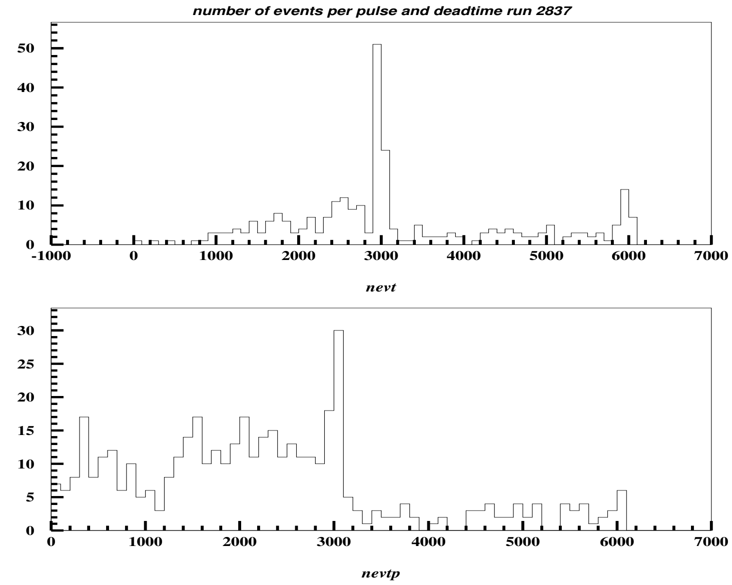

Fig 15. Peak spreads for run 2855. The upper plot is helicity plus while the bottom is helicity minus.

The correction (in the case of the "hadron" arm for example) applied to the asymmetry is:

$$T_3^i = T_{3_{with\ cut}}^i \cdot \frac{S_{hadron}^i}{T_{3_{no\ cut}}^i}$$

Where i is the helicity, T_3 is the number of triggers in the "hadron" arm and S is the corresponding scaler.

The Fig 16 and 17 are the plots for the 1.72 GeV asymmetries (second pass). The plot 15 is not deadtime corrected while the fig 16 is corrected. We can see that the deadtime effect is small but not negligible.

The Fig 17 and 18 are the plots for the 1.72 GeV asymmetries (third pass). The plot 17 is not deadtime corrected while the plot 18 is.

The Fig 20 plots the 0.862 GeV deadtime corrected asymmetries (to compare with fig 9).

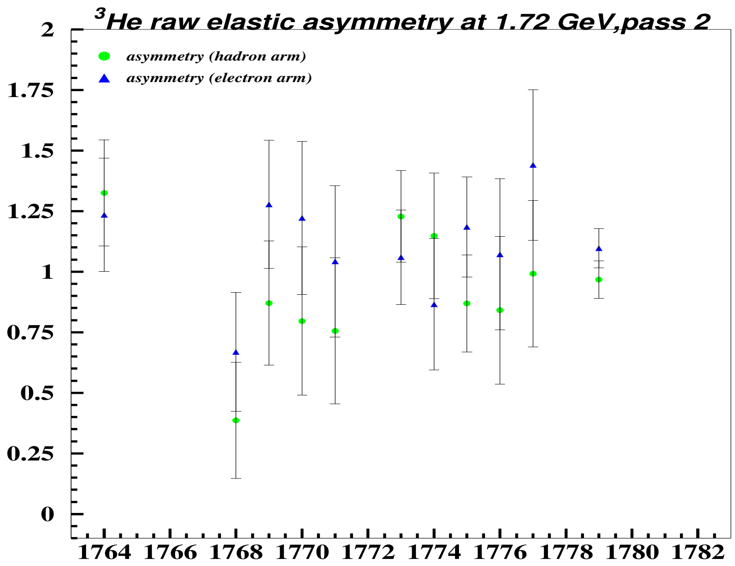

Fig 16 1.72 GeV asymmetries, first period. No deadtime correction.

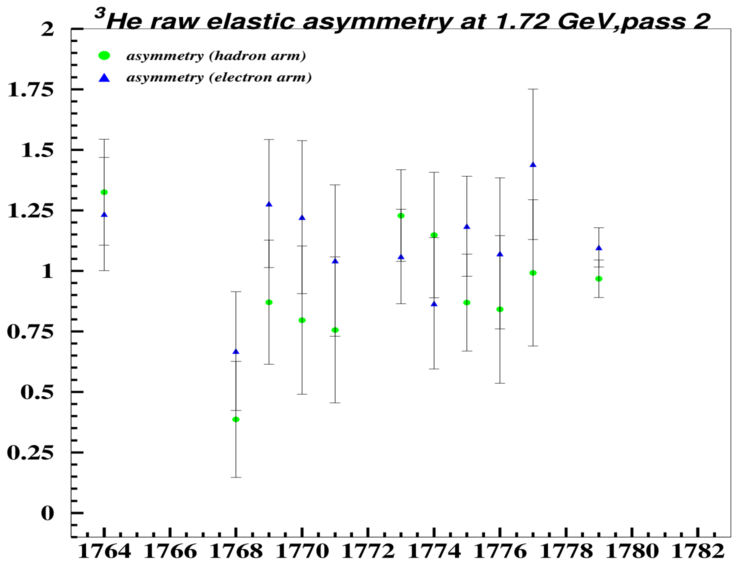

Fig 17 1.72 GeV asymmetries, first period. With deadtime correction.

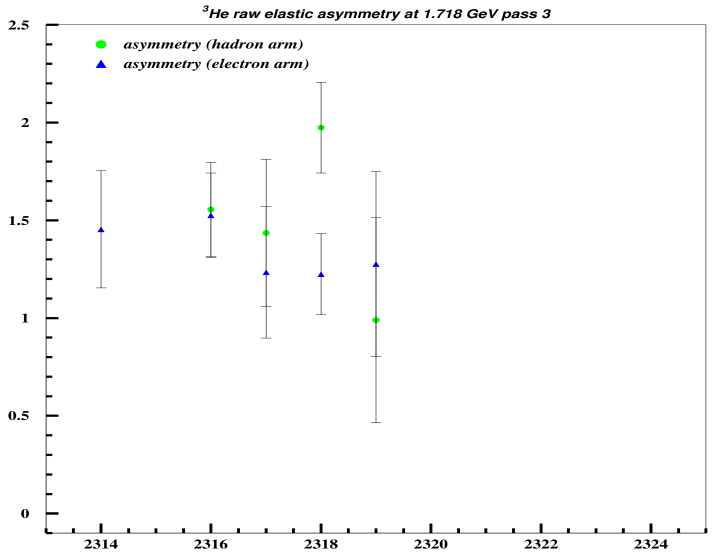

Fig 18 1.72 GeV asymmetries, second period. No deadtime correction.

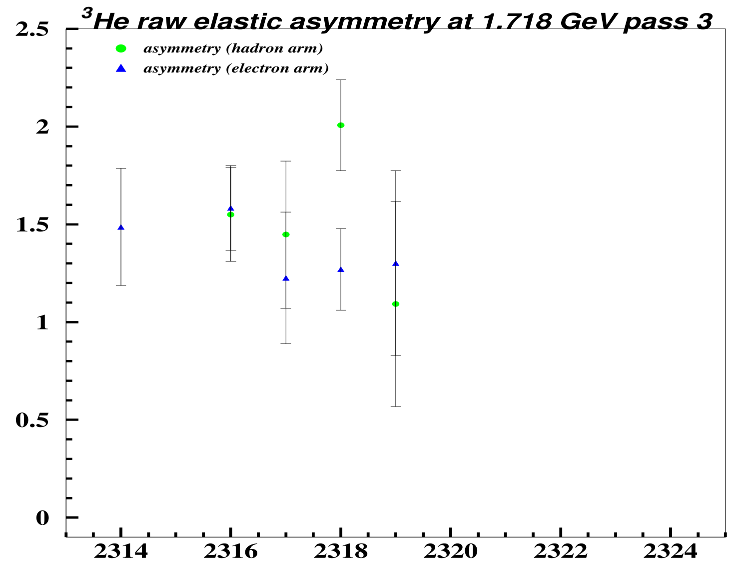

Fig 19 1.72 GeV asymmetries, second period. With deadtime correction.

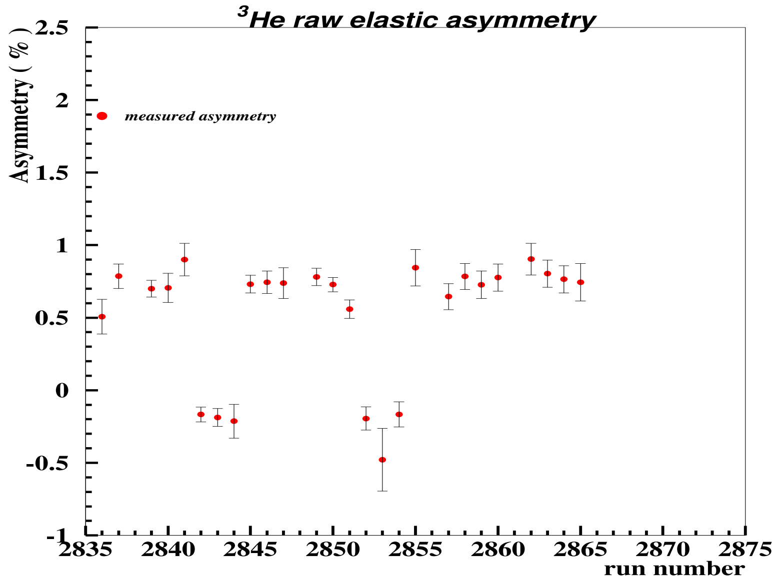

Fig 20 0.862 GeV asymmetries with deadtime correction.

4.5 Validity of the Correction.

The deadtime correction on the asymmetry can be several times larger than the asymmetry itself. Two tests check the consistency of the correction. The first is to see the correction effect by comparing the data before correction and after.

In addition of the elastic data this check was done on N_2 and ^{12}C unpolarised runs for both arms. The left plot in Figure 22 shows the uncorrected data for hadron arm. Average is zero since the target is unpolarised. On the left are the runs that do not need correction and on the right the ones needing to be corrected. The criteria is given by comparison of lifetime for both helicities (see Fig 10). If the lifetimes differ then a correction is needed. The x-axis display arbitrary run numbers. The right plot in fig. 22 shows the data after corrections of the runs on the right. We see that the data come back to a similar dispersion than the uncorrected data on the left.

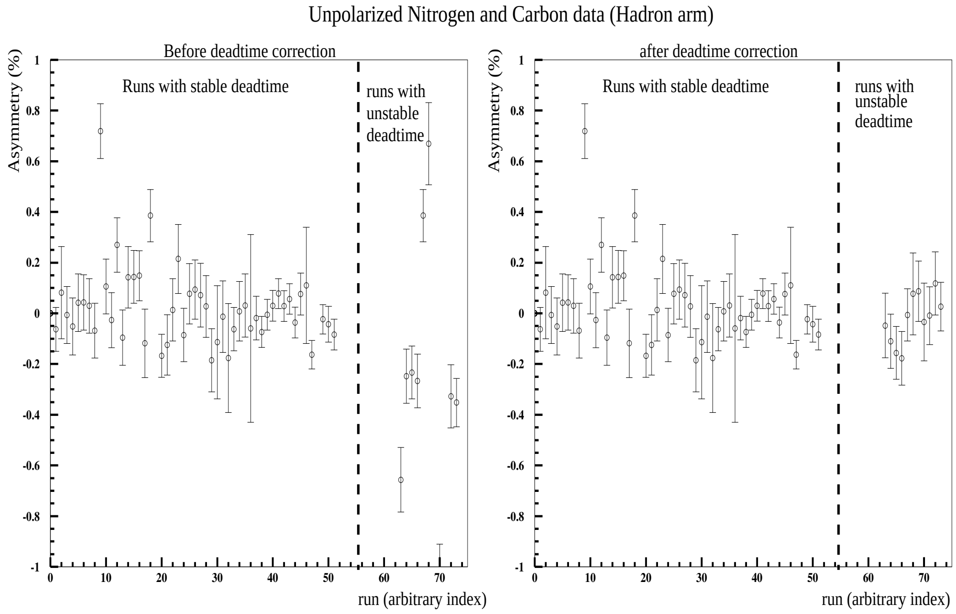

Fig 22. Unpolarised run asymmetries. On the right plot, the runs with unstable deadtime are corrected.

The asymmetry fluctuation, if all works properly, is due to statistic and should be random. The second test was to see if the asymmetry kept a Gaussian distribution. If another process adds to the asymmetry dispersion, then the distribution loses its Gaussian shape. The shape, after deadtime correction, was checked on ^{12}C and N_2 unpolarised runs. Fig. 23 shows the distribution of the corrected data on Hadron arm with a Gaussian fit. The fit matches well the data.

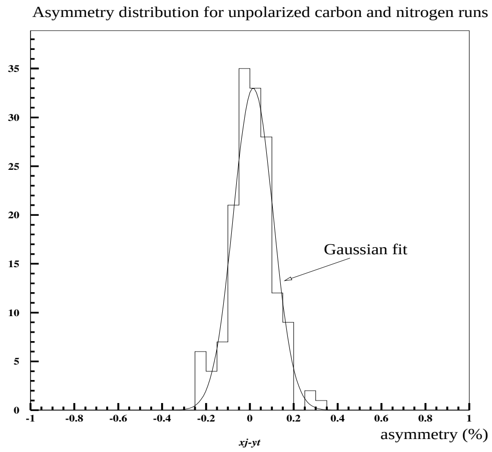

Fig 23. Helicity distribution for unpolarised runs fitted by a Gaussian.

These two checks were also conducted on electron arm data and provides similar results.

5 Helicity Assignation.

It is worth to mention the way the helicity is assigned to an event since it can biased the experimental asymmetry.

The signal coding the beam helicity information is a logical signal: A high value means a helicity plus type while a low value means the other. To avoid problems during the helicity flips of the beam, a 200 μs gate is settled during the flip. All the events coming during the gate have an undefined helicity and are cut away. The helicity signal coming from the accelerator is split in two ADCs.[8] An inversor before one of the ADC reverses the sign of the signal. A 2D plot of the two ADCs value then allows to select the helicity (see Fig 24). A hight value of one ADC with a low value of the other means an helicity type (the helicity type depends of the accelerator half-wave plate setup). The contrary means the other helicity type. Two low values of the ADCs means the beam helicity is flipping. A cut will be applied in this region (the 200 μs gate). Two high values of the ADCs should never happen. The table 1 sums up the helicity assignation.

ADC15	up	down	down	up
ADC16	down	down	up	up
helicity code	0	1	2	3
meaning	helicity+	undefined	helicity-	undefined

table 1. Helicity assignation

[8]In the case of "hadron" arm DAQ we have two other ADCs for redundancy information.

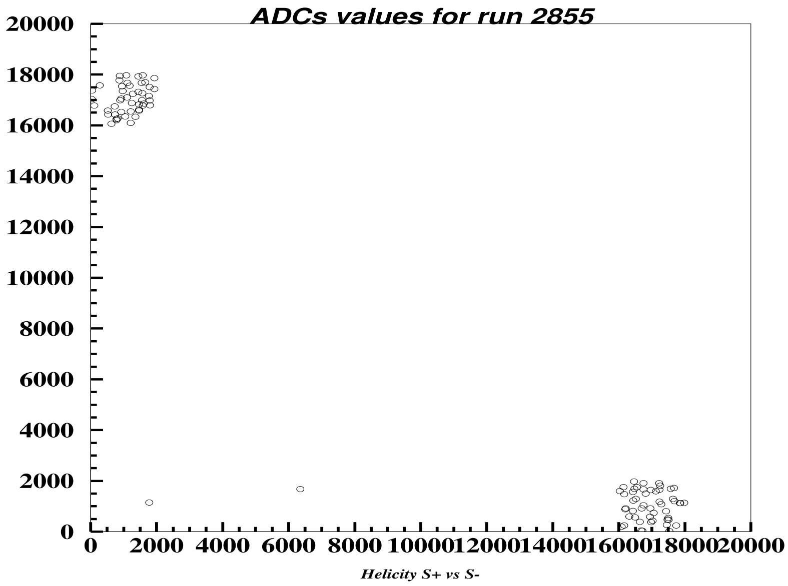

Fig 24. helicity ADCs value for run 2855.

If the ADCs cuts in fig 24 are unproper, they can biased the experimental results. For example if one ADC cut is much tighter than the other one, more events of this helicity will be recorded while they should have an undefined helicity. This was constantly monitored online. A check of the runs heavily affected by the deadtime-like problem shows the helicity assignation was properly done and was not the cause of the big jumps (see fig 9). No type 3 helicity events were found for these runs. For run 2855 79 type 1 helicity events were found which was close to the expected number (the run have 5.10^6 events, the pulse size is 1 s, the gate is about 200 μs that makes about 25 events coming during the gates. 36 other events correspond to scaler records and have also an undefined helicity that make 61 expected helicity 1 events, close the 79 registered). Other runs in this period were checked showing that the helicity was correctly monitored during the experiment and is not a concern for this analysis.

6 Systematic Error Estimate (preliminary).

we list the systematic errors on the asymmetry:

- Error on the target polarimetry: 5 %. [5]
- Error on the beam polarimetry: 2.7 %. [6]
- The error on the asymmetry due to a ± 2 MeV uncertainty on the beam energy is at worst 0.57 %. Hence it is neglected.
- The Nitrogen contamination is 0.7% for the 0.862 GeV elastic data. Hence the error on this number is negligible; The contamination for the 1.72 GeV elastic data is 8.5 %. We assume no significant error on this number since we used our experimental nitrogen data to compute it.

- The errors on the deadtime correction, acceptance, radiative correction and detector efficiency are neglected.
- We assume 2% error coming from the elastic form factor fit.
- Error on the asymmetry due to a ± 0.5 mRd uncertainty ([7]) on the spectrometer angle is about 1%.
- Error on the asymmetry due to a ± 1 degree on the target spin angle ([8]) is about 1% for the longitudinal asymmetry and 5.5% for the transverse one.

Added in quadrature we have a systematic error of 5.85 % for the longitudinal asymmetry and 7.97% for the transverse asymmetry.

Note In the next paragraph the error bars on the experimental results are the statistic one while the error bars on the simulated results are statistic.

7 Results.

The corrected experimental and expected asymmetries are compared in Fig 25, 26 and 27 for respectively 1.72 GeV first pass, 1.72 GeV second period and 0.862 GeV.

The Moller measurements of the beam polarisation were taken. The averaged NMR+EPR calibration for the target polarisation was used. They are applied to the expected asymmetry according to:

$A_{expected} = A_{theo}.P_{beam}.P_{target}$

Where P is the beam or target polarisation and A_{theo} is the expected asymmetry. The error bars on the experimental asymmetries are statistic. The last points on the plots are all the runs added together for the different passes.

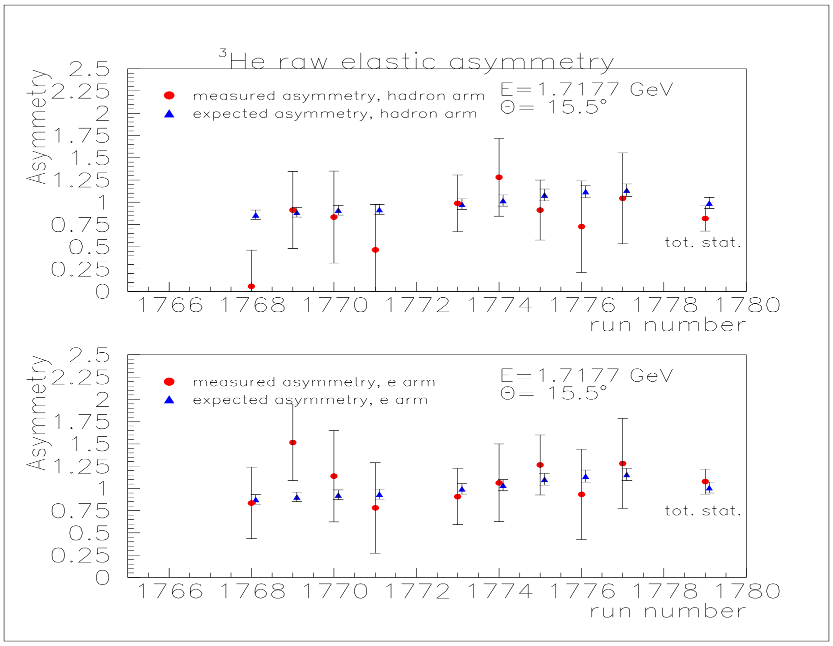

Fig 25. Corrected experimental and expected asymmetries for 1.72 GeV first period. The last points are all the runs summed together.

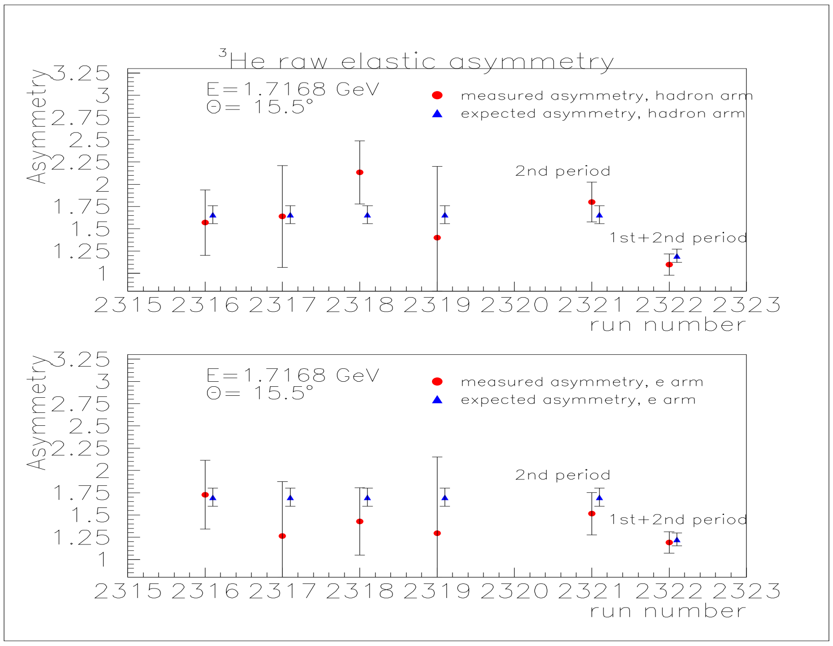

Fig 26. Corrected experimental and expected asymmetries for 1.72 GeV second period. The last points contains the full first and second periods statistic.

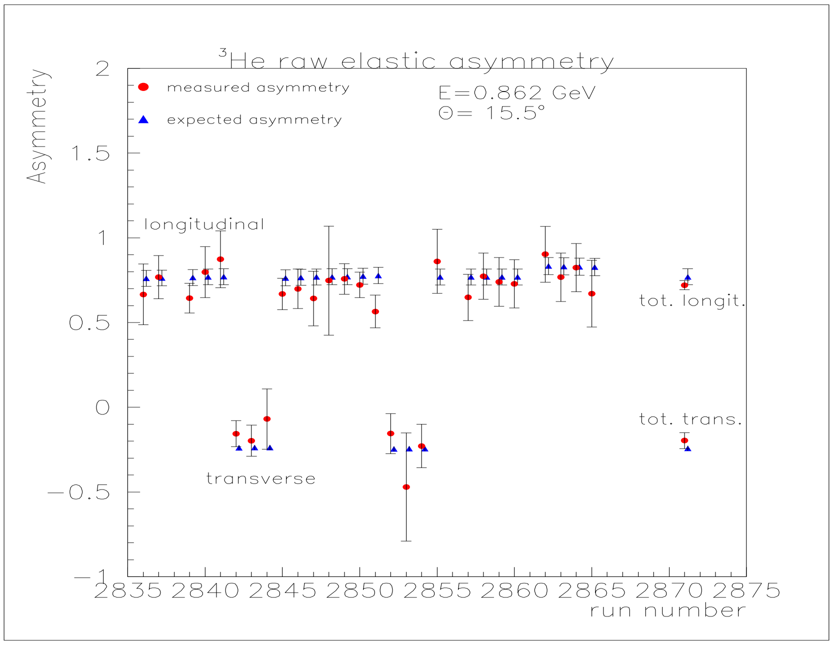

Fig 27. Corrected experimental and expected asymmetries for 0.862 GeV.

We summarize the results in the next tables. The first table gives the results for the “hadron” arm and the second table gives the electron arm results:

Energy	$A^{exp}_{\parallel}$ (%)	$A^{simu}_{\parallel}$ (%)	$A_{\perp}{}^{exp}$ (%)	$A_{\perp}{}^{simu}$ (%)
1.72 (period 1)	0.82±0.14	1.01±0.06	-	-
1.72 (period 2)	1.80±0.22	1.69±0.10	-	-
1.72 (1+2)	1.10±0.12	1.22±0.07	-	-
0.86	0.72±0.03	0.78±0.05	-0.20±0.05	-0.25±0.02

Table 2: Measured and simulated asymmetries for the “hadron” arm. Acceptance effect and dilution due to the fact that the beam and target are not fully polarized are folded in both experimental and simulated results. The uncertainty on the experimental results is only statistical while uncertainty on the simulation is systematic.

Energy	$A^{exp}_{\parallel}$ (%)	$A^{simu}_{\parallel}$ (%)
1.72 (period 1)	1.08±0.14	1.02±0.06
1.72 (period 2)	1.51±0.23	1.73±0.10
1.72 (1+2)	1.19±0.12	1.24±0.07

table 3: Same than previously but for electron arm.

8 Conclusion.

The experimental results at both energies agree with the expected ones within the errors bars. The systematic error achieved is about 6 %.

Acknowledgement. Thanks to David Lhuillier for his patient explanations and his work on the radiative corrections. Thanks also to Mark Jones and Bob Michael for the help on the deadtime problems and the useful suggestions.

References

[1] A. Deur: Wire Chamber analysis for E94010. E94010 technical note E94010TN29

[2] A. Deur: Single Arm Monte Carlo for Polarised ^{3}He experiment in Hall A. V.0.1. Hall A Technical Note in preparation.

[3] M. Vanderhaeghen *et al*: QED radiative correction to virtual Compton scattering

[4] A. Deur: Elastic Cross Section Analysis for E94010. E94010 technical note in preparation.

[5] S. Jensen. Ph. D. Thesis. Californian Institute of Technology.

[6] E. Chudakov. E94010 collaboration meeting, July 1999. (gen@jlab.org)

[7] N. Liyanage. E94010 collaboration meeting, May 2000. (nilanga@jlab.org)

[8] S. Incerti. Personal communication. (incerti@jlab.org)

[9] D. Lhuillier personal communication.